BJP BRITISH JOURNAL OF PHARMACOLOGY
BPS BRITISH PHARMACOLOGICAL SOCIETY

BJP British Journal of Pharmacology

DOI:10.1111/j.1476-5381.2010.00947.x
www.brjpharmacol.org

RESEARCH PAPER

Selective determinants of inositol 1,4,5-trisphosphate and adenophostin A interactions with type 1 inositol 1,4,5-trisphosphate receptors

Ana M Rossi[1], Kana M Sureshan[2]*, Andrew M Riley[2], Barry VL Potter[2] and Colin W Taylor[1]

[1]*Department of Pharmacology, University of Cambridge, Cambridge, UK, and* [2]*Wolfson Laboratory of Medicinal Chemistry, Department of Pharmacy and Pharmacology, University of Bath, Bath, UK*

Correspondence
Colin W. Taylor, Department of Pharmacology, University of Cambridge, Tennis Court Road, Cambridge CB2 1PD, UK. E-mail: cwt1000@cam.ac.uk

*Present address: Indian Institute of Science Education and Research, Thiruvananthapuram, Kerala-695016, India.

Keywords
adenophostin; Ca^{2+} signal; IP_3 receptor; structure–activity relationship

Received
8 March 2010
Revised
1 June 2010
Accepted
7 June 2010

BACKGROUND AND PURPOSE

Adenophostin A (AdA) is a potent agonist of inositol 1,4,5-trisphosphate receptors (IP_3R). AdA shares with IP_3 the essential features of all IP_3R agonists, namely structures equivalent to the 4,5-bisphosphate and 6-hydroxyl of IP_3, but the basis of its increased affinity is unclear. Hitherto, the 2′-phosphate of AdA has been thought to provide a supra-optimal mimic of the 1-phosphate of IP_3.

EXPERIMENTAL APPROACH

We examined the structural determinants of AdA binding to type 1 IP_3R (IP_3R1). Chemical synthesis and mutational analysis of IP_3R1 were combined with ^3H-IP_3 binding to full-length IP_3R1 and its N-terminal fragments, and Ca^{2+} release assays from recombinant IP_3R1 expressed in DT40 cells.

KEY RESULTS

Adenophostin A is at least 12-fold more potent than IP_3 in functional assays, and the IP_3-binding core (IBC, residues 224–604 of IP_3R1) is sufficient for this high-affinity binding of AdA. Removal of the 2′-phosphate from AdA (to give 2′-dephospho-AdA) had significantly lesser effects on its affinity for the IBC than did removal of the 1-phosphate from IP_3 (to give inositol 4,5-bisphosphate). Mutation of the only residue (R568) that interacts directly with the 1-phosphate of IP_3 decreased similarly (by ~30-fold) the affinity for IP_3 and AdA, but mutating R504, which has been proposed to form a cation-π interaction with the adenine of AdA, more profoundly reduced the affinity of IP_3R for AdA (353-fold) than for IP_3 (13-fold).

CONCLUSIONS AND IMPLICATIONS

The 2′-phosphate of AdA is not a major determinant of its high affinity. R504 in the receptor, most likely via a cation-π interaction, contributes specifically to AdA binding.

Abbreviations

AdA, adenophostin A; CLM, cytosol-like medium; IBC, IP_3-binding core; IP_2, inositol 4,5-bisphosphate; IP_3, inositol 1,4,5-trisphosphate; IP_3R, IP_3 receptor; K_d, equilibrium dissociation constant; n_{Hill}, Hill coefficient; NT, N-terminal; TEM, Tris/EDTA medium

Introduction

Receptors for inositol 1,4,5-trisphosphate (IP_3R, nomenclature follows Alexander *et al.*, 2009) are intracellular Ca^{2+} channels. They are expressed in the membranes of the endoplasmic reticulum of most animal cells (Foskett *et al.*, 2007) and they both initiate and propagate the Ca^{2+} signals evoked

by receptors that stimulate IP_3 formation (Berridge *et al.*, 2003). In vertebrates, three genes encode closely related subtypes of the IP_3R, which assemble into both homo- and hetero-tetrameric channels (Taylor *et al.*, 1999). The different subtypes share many features (Foskett *et al.*, 2007). Each subunit has a single IP_3-binding site towards the N-terminal, a large cytosolic regulatory domain, and six transmembrane domains, the last pair of which from each subunit, together with the intervening luminal loop, form the pore (Ramos-Franco *et al.*, 1999; Taylor *et al.*, 2004). For all IP_3R, IP_3 binding initiates the conformational changes that lead to opening of the channel. The IP_3-binding core [IBC, residues 224–604 of type 1 IP_3R (IP_3R1)] is entirely responsible for this initial recognition. The two domains (α and β) of the IBC form a clam-like structure lined with the basic residues that coordinate the phosphate groups of IP_3 (Bosanac *et al.*, 2002) (Figure 1A). The 4,5-bisphosphate and 6-hydroxyl groups of IP_3 are important for binding to IP_3R (Potter and Lampe, 1995), and each forms extensive interactions with the IBC. The 4-phosphate forms hydrogen bonds with several residues in the

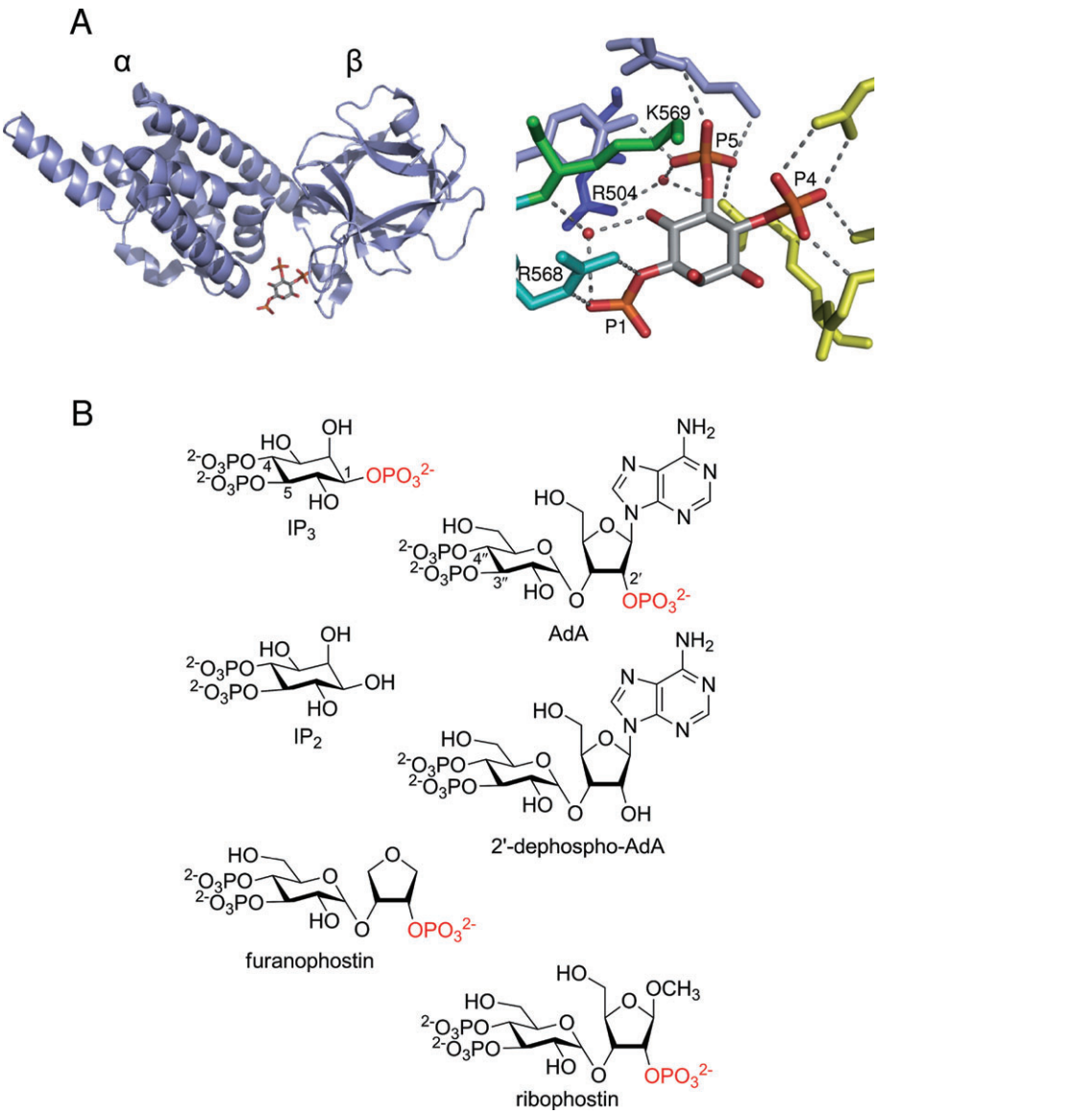

Figure 1

Structures of the IBC and the ligands used. Structure of the IBC (PDB 1N4K) with the enlarged panel highlighting the residues (R504, R568 and K569) mutated in this study and their interactions with the phosphate groups of IP_3. The red spheres represent water (A). Structures of the ligands used highlighting the 1-phosphate of IP_3 and 2′-phosphate of AdA (B). AdA, adenophostin A; IBC, IP_3-binding core; IP_3, inositol 1,4,5-trisphosphate.

β-domain, the 5-phosphate is hydrogen-bonded to residues predominantly within the α-domain and the 6-hydroxyl interacts indirectly via water with the backbone of K569 (Figure 1A). The 1-phosphate of IP_3 is not essential for binding to IP_3R, but it substantially increases the affinity of IP_3 (Nerou *et al.*, 2001); it interacts directly only with R568 and indirectly via a water molecule with the backbone of K569 (Bosanac *et al.*, 2002) (Figure 1A).

Adenophostins (Figure 1B) were originally isolated from *Penicillium brevicompactum* (Takahashi *et al.*, 1994a,b,c). They are potent agonists of IP_3R (Takahashi *et al.*, 1994b,c; Hirota *et al.*, 1995; Marchant *et al.*, 1997a; Shuto *et al.*, 1998; Correa *et al.*, 2001); they are not metabolized by the enzymes that degrade IP_3 and their structures are based on a glucose, rather than a *myo*-inositol, ring (Figure 1B). Adenophostin A (AdA) has proven a useful tool with which to explore the properties of IP_3R (Hirota *et al.*, 1995; Dellis *et al.*, 2006; Marchant and Parker, 1998; Yoshida *et al.*, 1998; Parekh *et al.*, 2002), and it has generated considerable interest in the synthesis of novel AdA analogues (Shuto *et al.*, 1998; Correa *et al.*, 2001; Borissow *et al.*, 2005; Mochizuki *et al.*, 2006).

Inositol 1,4,5-trisphosphate and AdA are each full agonists of the IP_3R (Rossi *et al.*, 2009). Both IP_3 and AdA bind to the IBC, and despite their structural differences, the 3″,4″-bisphosphate and 2″-hydroxyl groups of AdA evidently mimic the essential 4,5-bisphosphate and 6-hydroxyl of IP_3 (Figure 1B) (Takahashi *et al.*, 1994c; Hotoda *et al.*, 1999; Correa *et al.*, 2001; Rosenberg *et al.*, 2003). These features probably account for the binding of AdA to the IBC (Rosenberg *et al.*, 2003), but they do not explain the ability of AdA to bind to IP_3R with greater affinity than IP_3. Hitherto, a favoured suggestion is that the 2′-phosphate of AdA, which is thought to mimic the 1-phosphate of IP_3 (Figure 1B), is 'supra-optimally' positioned and thereby interacts more strongly with R568 and K569 than does the 1-phosphate of IP_3 (Takahashi *et al.*, 1994c; Wilcox *et al.*, 1995; Hotoda *et al.*, 1999). Alternatively, the adenine of AdA may interact directly with the IP_3R (Hotoda *et al.*, 1999; Glouchankova *et al.*, 2000; Rosenberg *et al.*, 2003). Such an interaction would need to be rather tolerant of changes to the adenine group because even substantial modifications to it cause only modest decreases in affinity (Correa *et al.*, 2001; Sureshan *et al.*, 2008). Defining the mechanisms responsible for high-affinity binding of AdA would both provide an important step towards rational development of ligands of the IP_3R with increased affinity, and contribute to resolving the mechanisms whereby IP_3 and AdA can have different effects on Ca^{2+} signalling (Rossi *et al.*, 2010). Here, we have used synthetic analogues of IP_3 and AdA and systematic mutagenesis of the IBC to address the structural basis of the high-affinity binding of AdA to IP_3R.

Methods

Stable expression of mutant IP_3R1 in DT40 cells

Cloning of rat IP_3R1 (without the S1 splice site) into the pENTR1A vector has been reported previously (Rossi *et al.*, 2009). The QuikChange II XL site-directed mutagenesis kit (Stratagene, La Jolla, CA, USA) was used to introduce point mutations into rat IP_3R1 using the primers (5′-3′) forward: TCA CAGCAAGACTACCAGAAGAACCAGGAGTAC, and reverse: GTACTCCTGGTTCTTCTGGTAGTCTTGCT GTGA for R568Q, and forward: TTCTCTAAGCCCAA CCAAGAGCGGCAGAAGCTG, and reverse: CAG CTTCTGCCGCTCTTGGTTGGGCTTAGAGAA for R504Q. The sequences of all mutant constructs were confirmed by sequencing of the full-length IP_3R. Mutated IP_3R were subcloned into the expression vector, pcDNA3.2/V5-DEST, by recombination (Invitrogen, Paisley, UK). DT40 cells stably expressing IP_3R1 and its mutants were generated by transfection of cells lacking endogenous IP_3R (Sugawara *et al.*, 1997). DT40 cells were cultured in RPMI 1640 medium supplemented with fetal bovine serum (10%), heat-inactivated chicken serum (1%), 2-mercaptoethanol (50 μM) and glutamine (2 mM). Cells were grown in suspension at 37°C in an atmosphere of 95% air and 5% CO_2, and passaged or used for Ca^{2+} experiments when they reached a density of ~2×10^6 cells·mL^{-1} (Tovey *et al.*, 2006). IP_3R expression was quantified by immunoblotting using an antiserum (Ab1.5) to a peptide corresponding to residues 2733–2749 of rat IP_3R1.

Mutagenesis of N-terminal fragments of IP_3R1

N-terminal fragments of IP_3R1 (IBC, residues 224–604; NT, residues 1–604) were amplified by PCR from the rat IP_3R1 clone lacking the S1 splice site and ligated into pTrcHisA vectors for expression of N-terminally tagged His_6 fusion proteins as previously described (Rossi *et al.*, 2009). The IBC included the S1 splice site, but the NT lacked it. The presence of the S1 splice site does not affect the equilibrium dissociation constant (K_d) of the IBC for IP_3 (data not shown). All fragments are numbered by reference to the full-length ($S1^+$) rat IP_3R1 (GenBank accession number: GQ233032.1). The QuikChange II XL site-directed mutagenesis kit was used to introduce point mutations into the IBC and NT constructs in pTrcHisA

vectors using the primers listed in the preceding section. The sequences of all constructs were confirmed.

Expression of fragments of IP_3R1

His_6-tagged IBC and NT fragments were expressed as described previously (Rossi *et al.*, 2009). Briefly, constructs were transformed into *E. coli* strain BL21(DE3). Cells were grown in Luria-Bertani medium containing ampicillin (100 $\mu g \cdot mL^{-1}$) at 22°C until the OD_{600} reached 1.0–1.5. The culture was then induced by addition of isopropyl β-D-thiogalactoside (0.5 mM), and after 20 h at 15°C, cells were harvested and lysates were prepared in Tris/EDTA medium (TEM: 50 mM Tris, 1 mM EDTA, pH 8.3) as described (Rossi *et al.*, 2009). Expression was detected by immunoblotting using an anti-His_6 antibody (Sigma, Poole, Dorset, UK). Proteins were cleaved from the His_6 tags by incubating bacterial lysate (6 h, 4°C) with thrombin (43 units$\cdot mg^{-1}$ bacterial protein) in phosphate-buffered saline. Cleavage was monitored by immunoblotting (Rossi *et al.*, 2009) using anti-His_6 antibody and antisera raised to peptides corresponding to residues 62–75 (Ab1) (Cardy *et al.*, 1997) or 326–343 (the SI splice site, Ab1.1) of IP_3R1 (Rossi *et al.*, 2009) for the NT and IBC respectively.

Purification of IP_3R from rat cerebellum

All animal care and experimental procedures complied with UK Home Office policy and with local animal regulations. Adult male Wistar rats were humanely killed by cervical dislocation and cerebella were removed, rapidly frozen in liquid nitrogen and stored at –80°C. IP_3R1 was purified from cerebella using heparin-affinity chromatography following a published protocol (Jiang *et al.*, 2002) with some modifications (Rossi *et al.*, 2009). Briefly, cerebella (2 g) were homogenized in homogenization medium [30 mL, HM: 1 M NaCl, 1 mM EDTA, 50 mM Tris, 1 mM benzamidine, Roche protease inhibitor cocktail (1 tablet per 25 mL), pH 8.3], and then centrifuged (100 000× *g*, 30 min). The pellet was solubilized in 20 mL of HM without NaCl, but supplemented with CHAPS (1.2%). After centrifugation (100 000× *g*, 1 h), the NaCl concentration of the supernatant was increased to 250 mM, and the supernatant was loaded onto heparin-agarose beads (5 mL). After 30 min, the beads were washed twice in glycerol-containing medium [250 mM NaCl, 50 mM Tris, 10% glycerol, 1 mM 2-mercaptoethanol, 1 mM benzamidine, 1 mM EGTA, 1% CHAPS, Roche protease inhibitor cocktail (1 tablet per 50 mL), pH 8.0]. IP_3R were eluted with elution medium (500 mM NaCl, 50 mM Tris, 10% glycerol, 1 mM 2-mercaptoethanol, 1 mM benzamidine, 1 mM EGTA, 50 mM Tris, 1% CHAPS, pH 8.0). Samples (~100 μg protein per mL) were frozen in liquid nitrogen and stored at –80°C.

^3H-IP_3 binding

Equilibrium-competition binding assays were performed as described (Rossi *et al.*, 2009). Briefly, incubations (500 μL) at 4°C were in either TEM or cytosol-like medium [CLM: 20 mM NaCl, 140 mM KCl, 1 mM EGTA, 20 mM PIPES, 2 mM $MgCl_2$, 375 μM $CaCl_2$ (free $[Ca^{2+}]$ = 220 nM), pH 7.0] containing ^3H-IP_3 (0.75–3 nM), bacterial lysate (~1–10 μg protein) or purified IP_3R1 (~2.5 μg), and competing ligands. For assays using full-length purified IP_3R, all media also included CHAPS (1%). Reactions were terminated after 5 min by addition of poly(ethylene glycol) 8000 (500 μL, 30%, w/v) and γ-globulin (30 μL, 25 $mg \cdot mL^{-1}$), followed by centrifugation (20 000× *g*, 5 min). Radioactivity was determined by liquid scintillation counting. Non-specific binding, determined by addition of 10 μM IP_3, or by extrapolation of competition curves to infinite IP_3 concentration, was <10% of total binding.

Ca^{2+} release by IP_3R

A low-affinity Ca^{2+} indicator (Mag-fluo-4) was used to monitor the free $[Ca^{2+}]$ within the intracellular Ca^{2+} stores of DT40 cells (Laude *et al.*, 2005; Tovey *et al.*, 2006). DT40 cells stably expressing IP_3R1 or its mutants were centrifuged (650× *g*, 2 min) and suspended in medium containing 135 mM NaCl, 5.9 mM KCl, 11.6 mM HEPES, 1.5 mM $CaCl_2$, 11.5 mM glucose, 1.2 mM $MgCl_2$, pH 7.3, 1 $mg \cdot mL^{-1}$ BSA, 0.4 $mg \cdot mL^{-1}$ Pluronic F127 and 20 μM Mag-fluo-4 AM. After 1 h at 20°C, cells were suspended in Ca^{2+}-free CLM supplemented with saponin (10 $\mu g \cdot mL^{-1}$) to allow selective permeabilization of the plasma membrane. Permeabilized cells were centrifuged (650× *g*, 2 min), re-suspended in CLM without Mg^{2+}, but supplemented with 10 μM carbonyl cyanide *p*-trifluoromethoxyphenylhydrazone (FCCP) to inhibit mitochondria, and 375 μM $CaCl_2$ to give a final free $[Ca^{2+}]$ of ~220 nM after addition of 1.5 mM MgATP. Cells (~5×10^5 cells per well) were attached to poly-L-lysine-coated, 96-well, black-walled plates (Greiner, Stonehouse, UK). Fluorescence was recorded at 20°C using a FlexStation III plate reader (MDS Analytical Technologies, Woking, Berks, UK) with excitation and emission wavelengths of 485 nm and 520 nm respectively. MgATP (1.5 mM) was added to initiate Ca^{2+} uptake, and when the endoplasmic reticulum had loaded to steady state with Ca^{2+}, IP_3, AdA or their analogues were added. Ca^{2+} release is expressed as a fraction of the ATP-dependent uptake (Tovey *et al.*, 2006).

Data analysis

Equilibrium binding results and concentration–effect relationships were fitted to Hill equations (GraphPad Prism, version 5) from which the Hill coefficients (n_{Hill}), –logIC_{50} (pIC_{50}) and –logEC_{50} (pEC_{50}) values were obtained. For equilibrium-competition binding assays, pK_d values were calculated using the Cheng and Prusoff equation (Cheng and Prusoff, 1973). Because pEC_{50} and pK_d values are normally distributed, these results are presented as means ± SEM from *n* independent experiments. For comparisons of the ratios between mean values (EC_{50} or K_d), statistical analyses compared the differences between their log values (ΔpEC_{50} or ΔpK_d) (Colquhoun, 1971) with the SEM calculated as follows, assuming that the population variances are the same (confirmed using an *F*-test) (Ott and Longnecker, 2010):

$$SEM = s_p\sqrt{\frac{1}{n_1}+\frac{1}{n_2}}$$

where, s_p. is the estimate of the population variance:

$$s_p = \sqrt{\frac{(n_1-1)s_1^2+(n_2-1)s_2^2}{n_1-n_2-2}}$$

where, s_1 and s_2 are the sample standard deviations, and n_1 and n_2 are the sample sizes.

Although all analyses were performed using log values, for greater clarity we present some ratios as the antilogs of the means ± SEM.

Statistical analysis used ANOVA followed by Bonferroni test for selected pairs, or unpaired Student's *t*-tests (GraphPad Prism, version 5). $P < 0.05$ was considered significant.

Materials

Protease inhibitor cocktail was from Roche (Burgess Hill, Sussex, UK). Heparin-agarose beads and sera were from Sigma (Poole, Dorset, UK). Thrombin was from GE Healthcare (Little Chalfont, Bucks, UK). CHAPS (3-[3-(cholamidopropyl) dimethylammonio]-1-propane-sulphonate) was from Helford Laboratories (Suffolk, UK). RPMI 1640 medium, Pluronic F127 and Mag-fluo-4 AM were from Invitrogen (Paisley, Scotland). ^{3}H-IP_3 (681 GBq·mmol^{-1}) was from PerkinElmer (Bucks, UK). IP_3 was from Alexis Biochemicals (Nottingham, UK). AdA (Borissow *et al.*, 2005), 2′-dephospho-AdA (Sureshan *et al.*, 2009), furanophostin (Marwood *et al.*, 1999) and ribophostin (Jenkins *et al.*, 1997) were synthesized as previously described. Inositol 4,5-bisphosphate (IP_2) was synthesized by hydrogenolytic deprotection of 1D-2,3,6-tri-*O*-benzyl-4,5-bis(dibenzyloxyphosphoryl) *myo*-inositol (Desai *et al.*, 1994). All ligands were purified by ion-exchange chromatography, fully characterized by the usual spectroscopic methods and accurately quantified by total phosphate assay. The structures of the ligands used are shown in Figure 1B. Sources of other reagents either are specified elsewhere in the methods or were previously reported (Rossi *et al.*, 2009).

Results

Stimulation of IP_3R1 by AdA

We used full-length IP_3R1 purified from rat cerebellum for binding assays, and DT40 cells expressing only recombinant IP_3R1 to measure Ca^{2+} release from intracellular stores. Most published analyses of ^{3}H-IP_3 binding use media similar to TEM because its high pH and/or low ionic strength reduce the K_d of IP_3R for IP_3, thereby increasing the specific binding determined with low concentrations of ^{3}H-IP_3. At the densities that recombinant full-length IP_3R are expressed, it is impracticable to measure ^{3}H-IP_3 binding in CLM, although it is feasible with the bacterially expressed fragments of IP_3R. To allow comparison with published work (Hirota *et al.*, 1995; Hotoda *et al.*, 1999; Glouchankova *et al.*, 2000; Rossi *et al.*, 2009) and to provide a direct comparison with our analyses of binding to IP_3R fragments, we first examined IP_3 and AdA binding to IP_3R1 in TEM.

In both binding (in TEM) and functional analyses (in CLM), AdA was ~12- to 19-fold more potent than IP_3 (ΔpK_d = 1.27 ± 0.09 and ΔpEC_{50} 1.09 ± 0.05) (Figure 2A and B, Table 1, Table S1). These results are consistent with many previous studies (Hirota *et al.*, 1995; Shuto *et al.*, 1998; Correa *et al.*, 2001; Morris *et al.*, 2002). We note, however, that in one series of studies (Takahashi *et al.*, 1994a,b,c), the K_d values for IP_3 and AdA were incorrectly calculated from the IC_{50}. The correct K_d for IP_3 and AdA calculated from the data provided are 13 nM and 0.73 nM, respectively, suggesting that in these studies too, AdA bound with about 18-fold greater affinity than IP_3, rather than the stated 100-fold difference.

Inositol 1,4,5-trisphosphate binding is entirely mediated by residues in the IBC (Bosanac *et al.*, 2002) (Figure 1A). We therefore compared IP_3 and AdA binding to the isolated NT, initially in TEM. The results, consistent with a previous analysis of a slightly shorter NT fragment of IP_3R1 (residues 1–580) (Glouchankova *et al.*, 2000), establish that the NT alone binds AdA with about 15-fold greater affinity (ΔpK_d = 1.18 ± 0.12) than IP_3 (Figure 2C, Table 2 and Table S1). To allow more direct

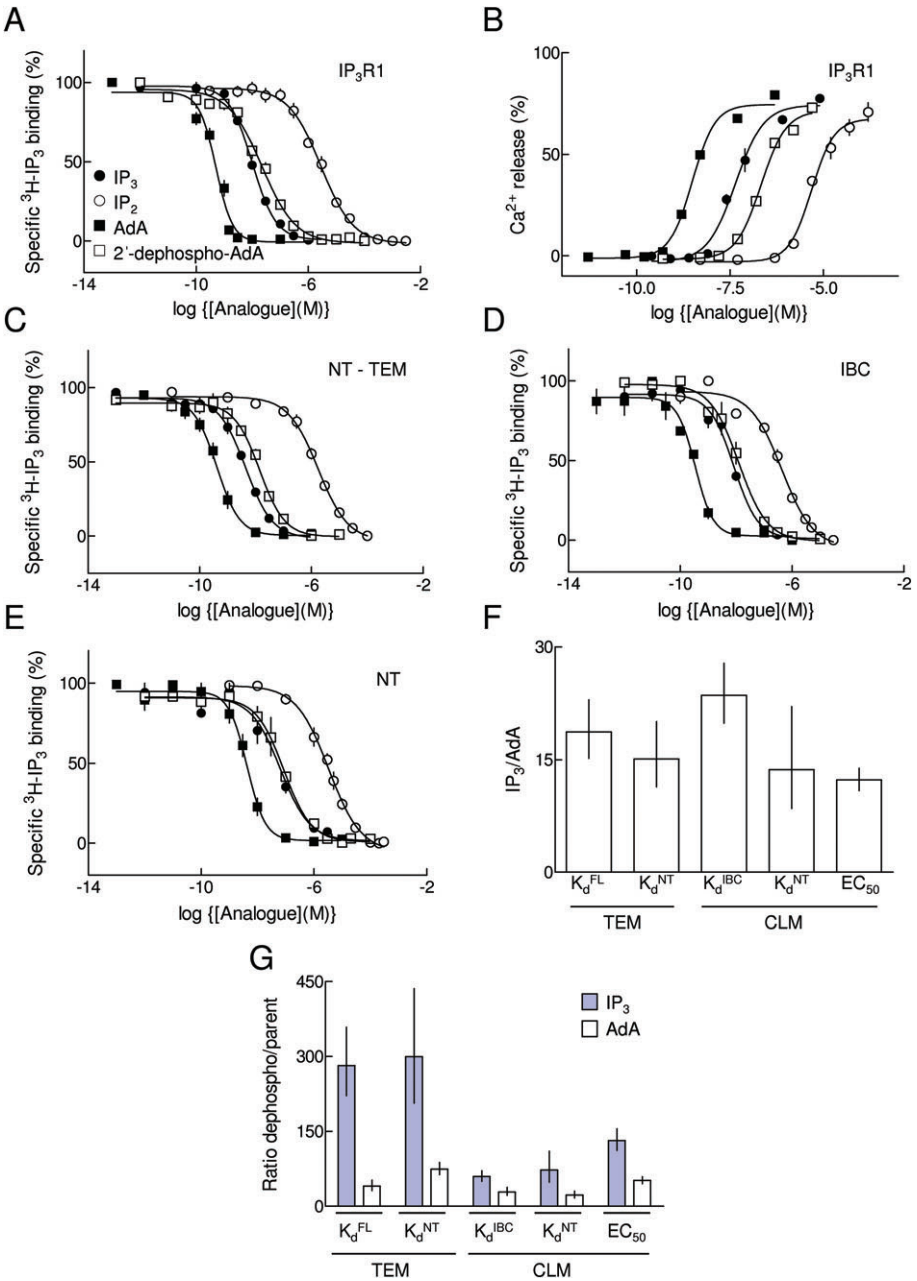

Figure 2

Interactions of AdA, IP_3, and their dephospho analogues with IP_3R and its N-terminal (NT) fragments. Equilibrium-competition binding to purified IP_3R1 using ^{3}H-IP_3 (1.5 nM) and the indicated ligands in TEM (A). Ca^{2+} release from permeabilized DT40-IP_3R1 cells evoked by the indicated ligands (B). Equilibrium-competition binding to the NT using ^{3}H-IP_3 (1.5 nM) and the indicated ligands in TEM (C). Equilibrium-competition binding to the IBC using ^{3}H-IP_3 (0.75 nM) and the indicated ligands in CLM (D). Equilibrium-competition binding to the NT using ^{3}H-IP_3 (1.5 nM) and the indicated ligands in CLM (E). The key to the symbols shown in panel A applies to all five panels (A–E). For each analysis (A–E) the K_d (from binding) or EC_{50} (from functional assays) is shown as a ratio for IP_3 versus AdA (F). For each analysis (A–E), the K_d or EC_{50} is shown as a ratio for the dephospho analogue relative to IP_3 or AdA (G). Results are means ± SEM, $n \geq 4$. DT40-IP_3R1 cells, DT40 cells stably expressing rat type 1 IP_3R. AdA, adenophostin A; CLM, cytosol-like medium; IP_3, inositol 1,4,5-trisphosphate; IP_3R, IP_3 receptor; K_d, equilibrium dissociation constant; TEM, Tris/EDTA medium.

comparisons with functional assays, we compared IP_3 and AdA binding to the isolated IBC and NT in CLM. These results confirm the expected substantial decrease in affinity for IP_3 in CLM (~20-fold relative to TEM). More importantly, they establish that in CLM the relative affinities for AdA and IP_3 are not significantly different for the IBC and NT (ΔpK_d = 1.37 ± 0.07 for the IBC, and 1.14 ± 0.21 for the NT)

Table 1

Responses of IP_3R1 to IP_3, AdA and their analogues

	Ca^{2+} release EC_{50} (nM) (pEC_{50} ± SEM) n_{Hill} ± SEM	Release (%)	Binding K_d (nM) (pK_d ± SEM) n_{Hill} ± SEM
IP_3	38.0 (7.42 ± 0.02) 1.1 ± 0.2	79 ± 3	8.5 (8.07 ± 0.03) 1.0 ± 0.1
IP_2	5012 (5.30 ± 0.08) 1.4 ± 0.2	73 ± 7	2394 (5.62 ± 0.08) 0.8 ± 0.1
AdA	3.1 (8.51 ± 0.05) 1.4 ± 0.1	78 ± 3	0.46 (9.34 ± 0.07) 1.5 ± 0.1
2′-dephospho-AdA	160 (6.80 ± 0.02) 1.3 ± 0.2	72 ± 3	18.5 (7.73 ± 0.09) 0.7 ± 0.1

From experiments similar to those shown in Figure 2A and B, the effects of each analogue on Ca^{2+} release from the intracellular stores of permeabilized DT40-IP_3R1 cells and on ^3H-IP_3 binding to full-length IP_3R1 (in TEM) are summarized. Mean EC_{50} and K_d values are shown together with means ± SEM for pEC_{50}, pK_d, Hill coefficients (n_{Hill}) and the percentage Ca^{2+} release. Results are from at least four independent experiments, with each Ca^{2+} release assay performed with three determinations.

AdA, adenophostin A; DT40-IP_3R1 cells, DT40 cells stably expressing rat type 1 IP_3R; IP_2, inositol 4,5-bisphosphate; IP_3, inositol 1,4,5-trisphosphate; IP_3R, IP_3 receptor; K_d, equilibrium dissociation constant; n_{Hill}, Hill coefficient; TEM, Tris/EDTA medium.

(Figure 2D and E, Table 3 and Table S1). Indeed in all our assays, the relative affinities of IP_3 and AdA for binding to the full-length receptor and its fragments, and their relative potencies in functional assays are not significantly different (Figure 2F, Table S1). It is noteworthy that the n_{Hill} for the interactions of AdA with IP_3R consistently tend to be greater than unity (see Tables 1–4), even when the interactions are with monomeric IBC or NT (Tables 2 and 3). We and others have reported similar observations previously (reviewed in Rossi *et al.*, 2010), although the underlying mechanism is unresolved.

These results, which establish that the IBC includes the structural determinants for high-affinity binding of AdA, provide our justification for using the IBC in subsequent experiments to explore the structural determinants of AdA binding. With the exception of Gly-268, the residues within the IBC that coordinate IP_3 are conserved between all three IP_3R subtypes (Bosanac *et al.*, 2002), and the IBC from each subtype binds IP_3 with the same affinity (Iwai *et al.*, 2006). This, together with evidence that AdA is more potent than IP_3 in cells that predominantly express each IP_3 receptor subtype (Rossi *et al.*, 2010), suggests that the results obtained from our subsequent analysis of IP_3R1 and the IBC from IP_3R1 are probably applicable also to IP_3R2 and IP_3R3.

The 2′-phosphate is not responsible for high-affinity binding of AdA

The suggestion that the 2′-phosphate of AdA provides a supra-optimal mimic of the 1-phosphate of IP_3 (Takahashi *et al.*, 1994c; Wilcox *et al.*, 1995; Hotoda *et al.*, 1999) predicts that removal of each phosphate moiety should more profoundly reduce the affinity of AdA for IP_3R relative to IP_3. We tested this prediction using synthetic IP_2 and 2′-dephospho-AdA (Figure 1B). In equilibrium-competition binding analyses with full-length IP_3R1 (in TEM), IP_2 bound with 282-fold lower affinity than IP_3 (ΔpK_d = 2.45 ± 0.10), whereas loss of the 2′-phosphate from AdA caused only a 41-fold decrease in affinity (ΔpK_d = 1.61 ± 0.11) (Figure 2A, Table 1 and Table S1). For the IBC in CLM, removal of the critical phosphate also more substantially reduced the affinity for IP_3 relative to AdA: IP_3 bound with 60-fold higher affinity than IP_2 (ΔpK_d = 1.78 ± 0.08), whereas the affinities of 2′-dephospho-AdA and AdA differed by only 29-fold (ΔpK_d = 1.46 ± 0.12) (Figure 2D, Table 3 and Table S1). Similar results were obtained with the NT in TEM and CLM (Figure 2C and E, Tables 2 and 3 and Table S1). In Ca^{2+} release assays, and consistent with the binding analyses, removal of the 1-phosphate from IP_3 more substantially reduced its potency than did removal

Table 2

Binding of IP_3, AdA and their analogues to the NT fragment of IP_3R1 and its mutants assayed in TEM

	K_d (nM) ($pK_d \pm$ SEM) $n_{Hill} \pm$ SEM NT	NT^{R568Q}	NT^{R504Q}
IP_3	2.14	41.7	35.6
	(8.67 ± 0.13)	(7.38 ± 0.07)	(7.45 ± 0.05)
	0.9 ± 0.1	0.7 ± 0.1	0.8 ± 0.1
IP_2	641	974	1250
	(6.19 ± 0.09)	(6.01 ± 0.12)	(5.90 ± 0.11)
	0.8 ± 0.1	0.8 ± 0.1	0.9 ± 0.2
AdA	0.14	2.81	16.5
	(9.85 ± 0.04)	(8.55 ± 0.06)	(7.78 ± 0.06)
	1.0 ± 0.1	1.3 ± 0.2	0.9 ± 0.1
2′-dephospho-AdA	10.5	13.7	345
	(7.98 ± 0.07)	(7.86 ± 0.04)	(6.46 ± 0.08)
	1.0 ± 0.1	0.7 ± 0.1	0.8 ± 0.1
Ribophostin	1.92	ND	40.5
	(8.72 ± 0.18)		(7.39 ± 0.02)
	0.9 ± 0.2		0.9 ± 0.1
Furanophostin	1.19	ND	52.5
	(8.92 ± 0.08)		(7.29 ± 0.03)
	1.0 ± 0.1		1.0 ± 0.1

From equilibrium-competition binding assays, the K_d, pK_d and Hill coefficients (n_{Hill}) values for each ligand are shown for the NT and NT mutants of IP_3R1 measured in TEM. Parallel experiments with mutant NT fragments in CLM were not practicable because of the low affinity of the interactions. Results are means (K_d) or means ± SEM (pK_d and n_{Hill}) from 4–14 independent experiments.
AdA, adenophostin A; CLM, cytosol-like medium; IP_2, inositol 4,5-bisphosphate; IP_3, inositol 1,4,5-trisphosphate; IP_3R, IP_3 receptor; K_d, equilibrium dissociation constant; ND, not determined; n_{Hill}, Hill coefficient; NT, N-terminal; TEM, Tris/EDTA medium.

of the 2′-phosphate from AdA (Figure 2B, Table 1 and Table S1). A previous study suggested that loss of the 2′-phosphate of AdA more profoundly affected the K_d (Takahashi *et al.*, 1994a). However, as stated above, the authors miscalculated the K_d from the IC_{50}, and it is impossible from the data presented to estimate the correct K_d for 2′-dephospho-AdA. We note, although it is unclear whether it contributes to their reported low affinity of 2′-dephospho-AdA for IP_3R, that these authors used 2′-dephospho-AdA produced enzymatically rather than by synthesis (Takahashi *et al.*, 1994a).

It is noteworthy that the disparity between the affinities of IP_3 and AdA and their dephospho analogues was exaggerated in TEM (Figure 2G). We have not further explored the more pronounced effect of TEM on binding of AdA and IP_3 relative to 2′-dephospho-AdA and IP_2 (Table 2). The high pH of TEM favours substantial deprotonation of the phosphate groups in all the ligands (Felemez *et al.*, 1999), perhaps thereby enhancing their binding to the IBC. The larger effect of TEM on binding of the trisphosphate ligands (IP_3 and AdA) may reflect a greater effect of the different media (pH, ionic strength, counter-ions) on the ionization states of these ligands relative to the bisphosphate ligands. The results do, however, highlight the necessity to examine ligand binding to IP_3R in medium resembling that used for functional analyses (e.g. CLM) if the functional and binding analyses are to be compared reliably.

Our demonstration that removal of the 1-phosphate from IP_3 reduces both affinity and potency significantly more than does removal of the 2′-phosphate from AdA (Figure 2G) is inconsistent with the notion that the high affinity of AdA results from its 2′-phosphate providing a supra-optimal mimic of the 1-phosphate of IP_3 (Takahashi *et al.*, 1994c).

Contributions of R568 to AdA and IP_3 binding

R568 within the α-domain of the IBC is the only residue to interact directly with the 1-phosphate of

Table 3

Binding of IP_3, AdA and their dephospho analogues to the NT, IBC and IBC mutants assayed in CLM

	K_d (nM) ($pK_d \pm$ SEM) $n_{Hill} \pm$ SEM NT	IBC	IBC^{R568Q}	IBC^{R504Q}
IP_3	47.0	7.23	271	96.8
	(7.33 ± 0.16)	(8.14 ± 0.05)	(6.57 ± 0.04)	(7.01 ± 0.02)
	0.8 ± 0.2	1.0 ± 0.1	1.6 ± 0.3	1.3 ± 0.2
IP_2	3433	432	1077	624
	(5.46 ± 0.09)	(6.37 ± 0.04)	(5.97 ± 0.09)	(6.21 ± 0.06)
	0.8 ± 0.1	0.8 ± 0.1	1.1 ± 0.3	1.2 ± 0.4
AdA	3.44	0.31	9.48	149
	(8.46 ± 0.11)	(9.51 ± 0.03)	(8.02 ± 0.09)	(6.83 ± 0.04)
	1.3 ± 0.2	1.3 ± 0.3	1.3 ± 0.6	1.5 ± 0.2
2′-dephospho-AdA	77.2	8.82	26.4	308
	(7.11 ± 0.08)	(8.05 ± 0.12)	(7.58 ± 0.06)	(6.51 ± 0.08)
	0.9 ± 0.4	0.8 ± 0.1	1.1 ± 0.3	1.8 ± 0.7

From equilibrium-competition binding assays, the K_d, pK_d and Hill coefficient (n_{Hill}) for each ligand are shown for the NT, IBC, IBC^{R568Q} and IBC^{R504Q} fragments of IP_3R1 in CLM. Results are means (K_d) or means ± SEM (pK_d and n_{Hill}) from 3–6 independent experiments.
AdA, adenophostin A; CLM, cytosol-like medium; IBC, IP_3-binding core; IP_2, inositol 4,5-bisphosphate; IP_3, inositol 1,4,5-trisphosphate; IP_3R, IP_3 receptor; K_d, equilibrium dissociation constant; n_{Hill}, Hill coefficient; NT, N-terminal.

Table 4

Functional responses of mutant IP_3R1

	IP_3R1 EC_{50} (μM) ($pEC_{50} \pm$ SEM) $n_{Hill} \pm$ SEM	Release (%)	IP_3R1^{R568Q} EC_{50} (μM) ($pEC_{50} \pm$ SEM) $n_{Hill} \pm$ SEM	Release (%)	IP_3R1^{R504Q} EC_{50} (μM) ($pEC_{50} \pm$ SEM) $n_{Hill} \pm$ SEM	Release (%)
IP_3	0.038	79 ± 3	1.19	39 ± 4	0.85	53 ± 6
	(7.42 ± 0.02)		(5.92 ± 0.06)		(6.07 ± 0.04)	
	1.1 ± 0.2		1.5 ± 0.3		1.0 ± 0.3	
IP_2	5.01	73 ± 7	8.05	53 ± 5	26	57 ± 6
	(5.30 ± 0.08)		(5.09 ± 0.07)		(4.58 ± 0.14)	
	1.4 ± 0.2		1.1 ± 0.2		0.9 ± 0.2	
AdA	0.003	78 ± 3	0.02	53 ± 3	0.60	61 ± 3
	(8.51 ± 0.05)		(7.70 ± 0.05)		(6.219 ± 0.002)	
	1.4 ± 0.1		1.0 ± 0.2		1.3 ± 0.2	
2′-dephospho-AdA	0.16	72 ± 3	0.26	43 ± 4	4.21	46 ± 1
	(6.80 ± 0.02)		(6.59 ± 0.07)		(5.38 ± 0.05)	
	1.3 ± 0.2		1.7 ± 0.4		1.9 ± 0.4	

From experiments similar to those shown in Figures 2B, 3E and 4F, Ca^{2+} release was measured in DT40 cells expressing only the indicated mutant IP_3R. Results show the pEC_{50}, EC_{50}, n_{Hill} and the maximal Ca^{2+} release evoked by each agonist. Results are presented as means (EC_{50}) or means ± SEM (pEC_{50}, n_{Hill} and percentage Ca^{2+} release) from 4–6 independent experiments, each with three determinations.
AdA, adenophostin A; IP_2, inositol 4,5-bisphosphate; IP_3, inositol 1,4,5-trisphosphate; IP_3R, IP_3 receptor; n_{Hill}, Hill coefficient.

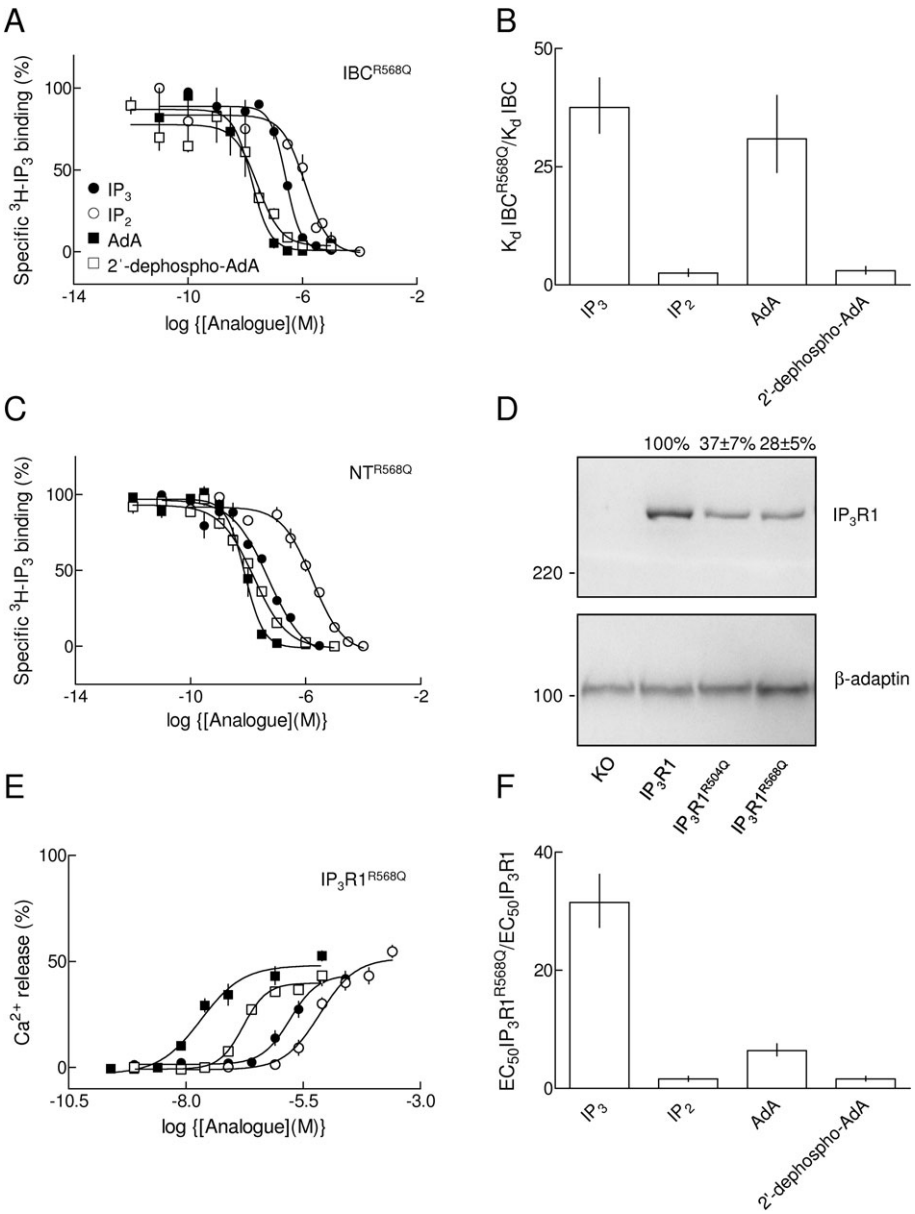

Figure 3

R568 does not selectively enhance AdA binding. Equilibrium-competition binding to IBC^{R568Q} using ^{3}H-IP$_3$ (1.5 nM) and the indicated ligands in CLM (A). Relative affinities (K_d) of ligands for the IBC^{R568Q} and IBC (B). Equilibrium-competition binding to the NT^{R568Q} using ^{3}H-IP$_3$ (1.5 nM) and the indicated ligands in TEM (C). Representative immunoblot (with anti-IP$_3$R1 antibody, Ab1.5, top panel; and β-adaptin, bottom panel) for DT40-KO cells (KO) and DT40 cells expressing IP$_3$R1 or the indicated mutants (10^5 cells per lane). Molecular weight markers (kDa) are shown. The blot is typical of six similar blots. IP$_3$R expression (corrected for β-adaptin loading) is shown for each mutant relative to DT40-IP$_3$R1 cells (%, means ± SEM) (D). Ca^{2+} release from permeabilized DT40-IP$_3$R1^{R568Q} cells evoked by the indicated ligands (E). Comparison of Ca^{2+} release for each ligand in normal and mutant IP$_3$R1^{R568Q} (F). Results are means ± SEM, $n \geq 4$. AdA, adenophostin A; CLM, cytosol-like medium; IBC, IP$_3$-binding core; IP$_3$, inositol 1,4,5-trisphosphate; IP$_3$R, IP$_3$ receptor; K_d, equilibrium dissociation constant; NT, N-terminal; TEM, Tris/EDTA medium.

IP$_3$, and it does so via two H-bonds with its side chain (Figure 1A) (Bosanac *et al.*, 2002). We mutated R568 to Q and examined IP$_3$ and AdA binding to the mutant IBC, and Ca^{2+} release via the mutant full-length IP$_3$R.

The affinities of IP$_3$ and AdA for the IBC were similarly reduced (by 37-fold and 31-fold respectively) by the R568Q mutation ($\Delta pK_d = 1.57 \pm 0.07$ for IP$_3$, and 1.49 ± 0.11 for AdA), whereas the affinities of IP$_2$ and 2′-dephospho-AdA were minimally affected ($\Delta pK_d = 0.40 \pm 0.14$ and 0.48 ± 0.12 for IP$_2$ and 2′-dephospho-AdA respectively) (Figure 3A and B, Table 3, Table S2). Similar results were obtained with NT^{R568Q} in TEM (Figure 3C, Table 2). These

results suggest that R568 recognizes the 1-phosphate of IP_3 and the 2′-phosphate of AdA similarly, and so lends further support to the view that the latter at least partially mimics the 1-phosphate of IP_3 (Figure 1B). But why, if IP_3 and AdA interact similarly with R568, should removal of the 1-phosphate from IP_3 increase its K_d more than does removal of the 2′-phosphate from AdA (Tables 1 and 2)? A likely explanation is that the indirect interaction of the 1-phosphate of IP_3 with the backbone of K569 (Figure 1A) (Bosanac *et al.*, 2002) is stronger than the equivalent interaction with the 2′-phosphate of AdA. Unfortunately, mutagenesis using naturally occurring amino acids cannot be used to dissect the role of this backbone interaction. Introduction of a non-natural amino acid, for example replacing K569 with an α-hydroxyl acid residue to replace the backbone NH with O, might address the question (Yang *et al.*, 2004). But the nonsense suppression techniques required to insert the non-natural residue are not presently available to us.

Functional assays of DT40 cells expressing mutant IP_3R do not allow absolute sensitivities to agonists or the size of the agonist-sensitive Ca^{2+} pool to be precisely compared between cell lines because it is impossible to establish stable cell lines with identical levels of IP_3R expression (Figure 3D). The problem is less severe than might have been anticipated because even a substantial increase in IP_3R expression in DT40 cells (>20-fold) caused the sensitivity to IP_3 to increase by less than twofold (Dellis *et al.*, 2006). The mutations we have studied caused much larger changes in IP_3 sensitivity (~30-fold, Table 4). Furthermore, levels of IP_3R expression in the stable DT40 cell lines expressing mutant IP_3R differed by no more than 3.5-fold from the line expressing wild-type IP_3R1 (Figure 3D).

In functional assays, using DT40 cells expressing only IP_3R1^{R568Q}, IP_3 and AdA were less potent than in cells expressing wild-type IP_3R1: the potencies of IP_3 and AdA were reduced by 31-fold (ΔpEC_{50} = 1.50 ± 0.06) and sixfold (ΔpEC_{50} = 0.81 ± 0.07) respectively. By contrast, the potencies of IP_2 and 2′-dephospho-AdA were only very modestly reduced (1.6-fold, ΔpEC_{50} = 0.21 ± 0.11 for both ligands) (Figure 3E and F, Table 4 and Table S3). The lesser Ca^{2+} release with maximally effective concentrations of all four agonists in DT40-IP_3R^{R568Q} cells (compare Figures 2B and 3E) is probably attributable to the reduced level of expression of IP_3R in the mutant cell line (Figure 3D). The selective effect of the R568Q mutation on AdA and IP_3, but not the dephospho analogues, is consistent with our analyses of ligand binding (Table 3). But the significantly lesser effect of the mutation on the functional responses to AdA was unexpected because hitherto the interactions between R568 have appeared similar for the 1-phosphate of IP_3 and the 2′-phosphate of AdA. These results suggest that disruption of the interaction between R568 and the critical phosphates may selectively reduce the efficacy of IP_3. That conclusion would be consistent with evidence that inositol 2,4,5-trisphosphate is a partial agonist of IP_3R (Marchant *et al.*, 1997b).

Selective interaction of AdA with R504

Our previous attempts to predict the binding mode of AdA to the IBC using molecular docking suggested that, in addition to possible interactions with R568, the 2′-phosphate might also interact with the amide NH of K569 and the side chain of R504 (Rosenberg *et al.*, 2003). But our present results (Figure 2) suggest that for AdA, the 2′-phosphate is not a major determinant of its high affinity. One of the possible binding modes also suggested a cation-π interaction between the adenine of AdA and the guanidinium side chain of R504 (Rosenberg *et al.*, 2003) (Figure 4A). Many analyses of synthetic AdA analogues lacking the adenine moiety suggest that the adenine or another aromatic moiety is an important determinant of the high-affinity binding of AdA. The AdA analogues lacking adenine, which retain a phosphate group equivalent to the 2′-phosphate of AdA, typically have K_d values similar to that for IP_3 (Table 2) (Jenkins *et al.*, 1997; Tatani *et al.*, 1998; Hotoda *et al.*, 1999; Marwood *et al.*, 2000; Correa *et al.*, 2001). R504 is one of several residues to form a hydrogen bond with the 5-phosphate of IP_3, via a bridging water molecule (Bosanac *et al.*, 2002), and probably also with the equivalent 3″-phosphate of AdA (Rosenberg *et al.*, 2003) (Figure 1B). Mutation of R504 inhibits IP_3 binding (Yoshikawa *et al.*, 1996) and is likewise expected to disrupt interaction of the 3″-phosphate of AdA. But if the proposed cation-π interaction is important for AdA binding, mutation of R504 might additionally reduce AdA binding by disrupting interactions with its adenine ring. The subsequent experiments were designed to test this hypothesis.

As expected, because each ligand has a phosphate equivalent to the 5-phosphate of IP_3, mutation of R504 to Q significantly reduced the affinity of both IP_3 and AdA for the IBC (Figure 4B and C, Table 3 and Table S3). However, whereas the affinity of IP_3 was reduced by 13-fold (ΔpK_d = 1.13 ± 0.06), the affinity of AdA was reduced by 353-fold (ΔpK_d = 2.55 ± 0.05) (Figure 4B and C, Table 3 and Table S2). Binding of the dephospho analogues was less affected by the R504Q mutation: the decrease in affinity was 1.4-fold (pΔ = 0.16 ± 0.07) for IP_2 and

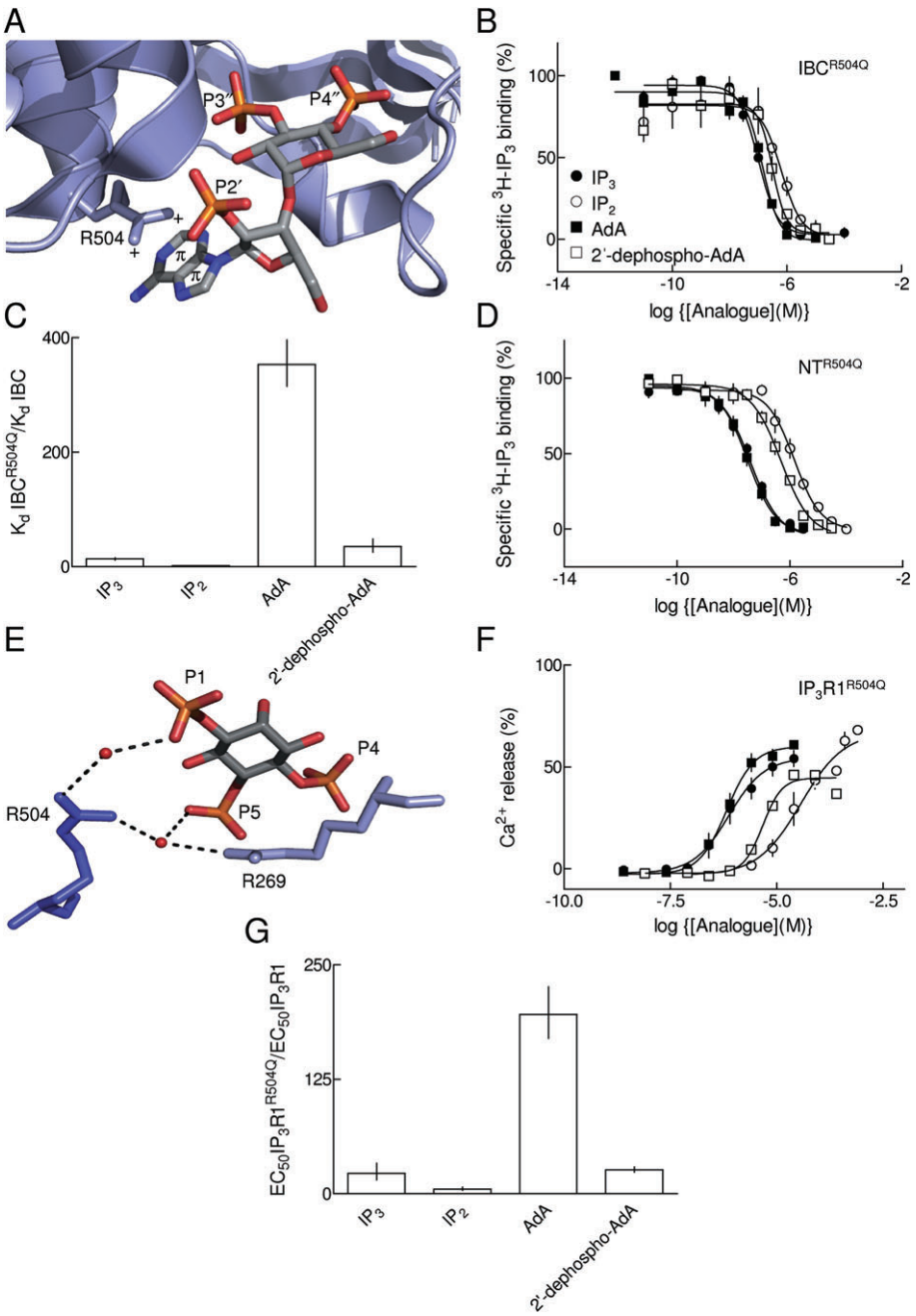

Figure 4

Selective interaction of AdA with R504. Model of AdA binding to the IBC highlighting a possible cation-π interaction between the adenine ring of AdA and R504 of the IBC (Rosenberg *et al.*, 2003) (A). Equilibrium-competition binding to IBC^{R504Q} using ^{3}H-IP_3 (3 nM) and the indicated ligands in CLM (B). Comparison of the binding of each ligand to normal and mutant IBC (C). Equilibrium-competition binding to NT^{R504Q} using ^{3}H-IP_3 (1.5 nM) and the indicated ligands in TEM (D). Structure of the IBC (PDB 1N4K) highlighting the likely interactions of R504 with the phosphate groups of IP_3 (see text for further details). The red spheres represent water (E). Ca^{2+} release from permeabilized IP_3R1^{R504Q} cells evoked by the indicated ligands (F). Comparison of Ca^{2+} release for each ligand via normal and mutant IP_3R (G). Results (B–D and F–G) are means ± SEM, $n \geq 4$. AdA, adenophostin A; CLM, cytosol-like medium; IBC, IP_3-binding core; IP_3, inositol 1,4,5-trisphosphate; IP_3R, IP_3 receptor; NT, N-terminal; TEM, Tris/EDTA medium.

35-fold ($\Delta pK_d = 1.54 \pm 0.14$) for 2′-dephospho-AdA. Similar results were obtained with NT^{R504Q} in TEM (Figure 4D, Table 2).

A further prediction arising from our suggestion that a cation-π interaction involving R504 and the adenine moiety contributes to high-affinity binding of AdA is that adenophostin analogues lacking the adenine moiety should be less affected by mutation of R504. The results shown in Table 2 confirm this prediction for two such analogues, furanophostin

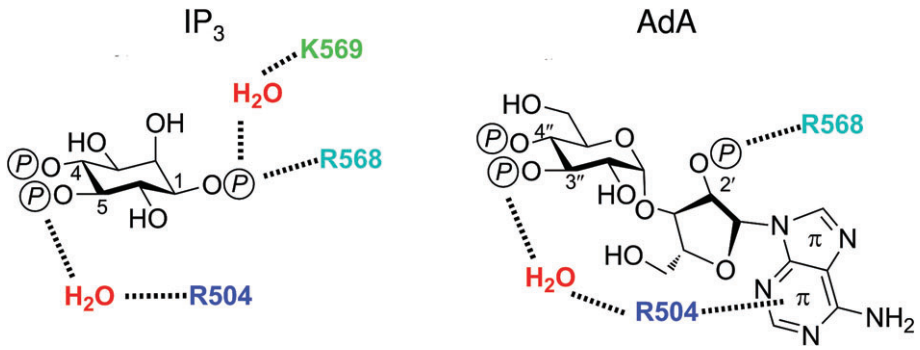

Figure 5

Differential interactions of IP_3 and AdA with the IBC. Interactions of the phosphate groups of IP_3 with the residues mutated in this study are highlighted (Bosanac *et al.*, 2002). Predicted interactions of the phosphate groups of AdA with the same residues, and the proposed cation-π interaction between the adenine moiety and R504 are shown. AdA, adenophostin A; IBC, IP_3-binding core; IP_3, inositol 1,4,5-trisphosphate.

and ribophostin (Figure 1B). Mutation of R504 to Q reduced the affinity of the NT for furanophostin by 44-fold ($\Delta pK_d = 1.63 \pm 0.10$) and for ribophostin by 21-fold ($\Delta pK_d = 1.33 \pm 0.24$).

Comparison of the effects of the R504Q mutation on each pair of ligands (i.e. IP_3 vs. AdA, and IP_2 vs. dephospho-AdA) indicates that for each there was a 25-fold greater decrease in the affinity for the AdA analogues (Figure 4C, Table 3 and Table S2). But the lesser effects of the mutation on both dephospho analogues is intriguing because R504 has not been reported to interact with the 1-phosphate of IP_3 (Bosanac *et al.*, 2002). However, close inspection of the crystal structure of the IP_3-bound IBC also reveals a possible indirect interaction, via water, of R504 with the 1-phosphate (Figure 4E), although this was not discussed in the original report (Bosanac *et al.*, 2002). It is not clear whether a similar interaction could also exist for AdA, but the possibility that both IP_3 and AdA interact with R504 via their 1- and 2′-phosphates, respectively, is appealing because it would explain the lesser effects of the R504Q mutation on the dephospho analogues (Figure 4C).

Functional analyses with DT40 cells expressing IP_3R1^{R504Q} confirmed the results with binding. The sensitivity of the mutant IP_3R1^{R504Q} was significantly decreased for all ligands, although again the effect on the dephospho analogues was more modest than that on IP_3 and AdA (Figure 4F and G, Table 4 and Table S3). Most importantly, whereas the EC_{50} for IP_3 was reduced by 23-fold ($\Delta pEC_{50} = 1.35 \pm 0.17$), that for AdA was reduced by 196-fold ($\Delta pEC_{50} = 2.29 \pm 0.06$). These ΔpEC_{50} values for IP_3 and AdA are significantly different. Together, the binding and functional analyses establish that R504 is more important for binding of AdA than for IP_3. The selective effect of R504 on AdA binding does not result from interaction with the 2′-phosphate of AdA, but is instead likely to reflect the contribution of a cation-π interaction between the adenine of AdA and the guanidinium side chain of R504 (Figure 4A).

Discussion

Inositol 1,4,5-trisphosphate and AdA are full agonists of IP_3R (Rossi *et al.*, 2009), but the latter binds with substantially greater affinity than does IP_3 (Takahashi *et al.*, 1994b; Correa *et al.*, 2001) (Figure 2F). We have established that the IBC, to which IP_3 binds to initiate activation of the IP_3R, is alone capable of binding AdA with ~20-fold greater affinity than IP_3 (Table 3). Presently available evidence suggests that once AdA or IP_3 has bound to the IBC, each causes indistinguishable activation of the IP_3R (Rossi *et al.*, 2009). The increased potency of AdA, relative to IP_3, in evoking Ca^{2+} release via IP_3R is therefore likely to be entirely attributable to the stronger interactions between AdA and the IBC. This conclusion provided the impetus for resolving the interactions between AdA and the IBC that mediate its high-affinity binding.

The 4″- and 3″-phosphates of AdA mimic the essential 4,5-bisphosphate moiety of IP_3 (Figure 1B) and the 2′-phosphate of AdA has been thought to at least partially mimic the 1-phosphate of IP_3 (Takahashi *et al.*, 1994b). None of our present results challenges this interpretation. Hitherto, an appealing explanation for the high affinity of AdA has been the suggestion that its 2′-phosphate is better placed than the 1-phosphate of IP_3 to interact with residues in the IBC (Takahashi *et al.*, 1994c; Wilcox *et al.*, 1995). Our results establish that this is not the basis of the high-affinity binding of AdA. First, removal of the 2′-phosphate

from AdA has significantly less effect on its activity than does removal of the 1-phosphate from IP_3 (Figure 2G, Tables 1–3 and Table S1). Second, mutation of R568, one of the key residues with which the 1-phosphate of IP_3 interacts (Bosanac *et al.*, 2002), similarly reduces the affinity of the IP_3R for IP_3 and AdA, while minimally affecting binding of IP_2 or 2′-dephospho-AdA (Figure 3A and B, Table 3 and Table S1). These results establish that the 2′-phosphate of AdA partially mimics the 1-phosphate of IP_3, but the latter probably interacts more strongly with the backbone of K569. We conclude that the high affinity of AdA for IP_3R does not result from its 2′-phosphate behaving as a supra-optimally positioned mimic of the 1-phosphate of IP_3 (Figure 5).

Considerable evidence suggests that the adenine group of AdA contributes significantly to its high-affinity binding (Tatani *et al.*, 1998; Hotoda *et al.*, 1999; Marwood *et al.*, 2000; Correa *et al.*, 2001; Rosenberg *et al.*, 2003) and our molecular modelling has suggested that this might result from a cation-π interaction between the adenine and the guanidinium side chain of R504 (Rosenberg *et al.*, 2003) (Figure 4A). Our present results are consistent with this suggestion. Because R504 interacts with the 5-phosphate of IP_3 (Figure 1A) and, almost certainly, in similar fashion with the equivalent 3″-phosphate of AdA (Figures 1B and 5), mutation of this residue (R504Q) significantly decreased the affinity of the IP_3R for both ligands. But more importantly, the effects, in both functional and binding assays, were significantly greater for AdA than for IP_3 (Figure 4D and G, Tables 2–4, Tables S2 and S3). These results establish the greater importance of R504 for AdA binding, which would be consistent with AdA, but not IP_3, forming a cation-π interaction with this residue (Figure 5). We conclude that the high affinity of AdA for IP_3R is not due to its 2′-phosphate, and that AdA interacts more strongly than IP_3 with R504, most likely reflecting a cation-π interaction between the adenine group and R504. This interaction may provide opportunities for synthesis of less polar ligands of IP_3R (Sureshan *et al.*, 2009).

Acknowledgements

This work was supported by grants from the Wellcome Trust to C.W.T. [085295] and B.V.L.P and A.M. Riley [082837]. A.M. Rossi is a fellow of Queens' College, Cambridge. We thank Stephen Hladky (Department of Pharmacology, Cambridge) for helpful comments on statistical analyses.

Conflicts of interest

None.

References

Alexander SPH, Mathie A, Peters JA (2009). Guide to Receptors and Channels, 4th edition. Br J Pharmacol 158: S1–S254.

Berridge MJ, Bootman MD, Roderick HL (2003). Calcium signalling: dynamics, homeostasis and remodelling. Nat Rev Mol Cell Biol 4: 517–529.

Borissow CN, Black SJ, Paul M, Tovey SC, Dedos SG, Taylor CW *et al.* (2005). Adenophostin A and analogues modified at the adenine moiety: synthesis, conformational analysis and biological activity. Org Biomol Chem 3: 245–252.

Bosanac I, Alattia J-R, Mal TK, Chan J, Talarico S, Tong FK *et al.* (2002). Structure of the inositol 1,4,5-trisphosphate receptor binding core in complex with its ligand. Nature 420: 696–700.

Cardy TJA, Traynor D, Taylor CW (1997). Differential regulation of types 1 and 3 inositol trisphosphate receptors by cytosolic Ca^{2+}. Biochem J 328: 785–793.

Cheng Y-C, Prusoff WH (1973). Relationship between the inhibition constant (K_I) and the concentration of inhibitor causing 50 per cent inhibition (IC_{50}) of an enzymatic reaction. Biochem Pharmacol 22: 3099–3108.

Colquhoun D (1971). Lectures in Biostatistics. Clarendon Press: Oxford.

Correa V, Riley AM, Shuto S, Horne G, Nerou EP, Marwood RD *et al.* (2001). Structural determinants of adenophostin A activity at inositol trisphosphate receptors. Mol Pharmacol 59: 1206–1215.

Dellis O, Dedos S, Tovey SC, Rahman T-U-, Dubel SJ, Taylor CW (2006). Ca^{2+} entry through plasma membrane IP_3 receptors. Science 313: 229–233.

Desai T, Gigg J, Gigg R, Martin-Zamora E (1994). The preparation of intermediates for the synthesis of 1D-*myo*-inositol 1,4,5- and 2,4,5-trisphosphates, 1,4-bisphosphate 5-phosphorothioate, and 4,5-bisphosphate 1-phosphorothioate from 1D-3,6-di-*O*-benzyl-1,2-*O*-isopropylidene-*myo*-inositol. Carbohydr Res 262: 59–77.

Felemez M, Marwood RD, Potter BVL, Spiess B (1999). Inframolecular studies of the protonation of adenophostin A: comparison with 1-D-*myo*-inositol 1,4,5-trisphosphate. Biochem Biophys Res Commun 266: 334–340.

Foskett JK, White C, Cheung KH, Mak DO (2007). Inositol trisphosphate receptor Ca^{2+} release channels. Physiol Rev 87: 593–658.

Glouchankova L, Krishna UM, Potter BVL, Falck JR, Bezprozvanny I (2000). Association of the inositol-(1,4,5) trisphosphate receptor ligand binding

site with phosphatidylinositol (4,5)-bisphosphate and adenophostin A. Mol Cell Biol Res Commun 3: 153–158.

Hirota J, Michikawa T, Miyawaki A, Takahashi M, Tanzawa K, Okura I *et al*. (1995). Adenophostin-mediated quantal Ca^{2+} release in the purified and reconstituted inositol 1,4,5-trisphosphate receptor type 1. FEBS Lett 368: 248–252.

Hotoda H, Murayama K, Miyamoto S, Iwata Y, Takahashi M, Kawase Y *et al*. (1999). Molecular recognition of adenophostin, a very potent Ca^{2+} inducer, at the D-*myo*-inositol 1,4,5-trisphosphate receptor. Biochemistry 38: 9234–9241.

Iwai M, Michikawa T, Bosanac I, Ikura M, Mikoshiba K (2006). Molecular basis of the isoform-specific ligand-binding affinity of inositol 1,4,5-trisphosphate receptors. J Biol Chem 282: 12755–12764.

Jenkins DJ, Marwood RD, Potter BVL (1997). A disaccharide polyphosphate mimic of 1D-*myo*-inositol 1,4,5-trisphosphate. Chem Commun 5: 449–450.

Jiang Q-X, Thrower EC, Chester DW, Ehrlich BE, Sigworth FJ (2002). Three-dimensional structure of the type 1 inositol 1,4,5-trisphosphate receptor at 24 Å resolution. EMBO J 21: 3575–3581.

Laude AJ, Tovey SC, Dedos S, Potter BVL, Lummis SCR, Taylor CW (2005). Rapid functional assays of recombinant IP_3 receptors. Cell Calcium 38: 45–51.

Marchant JS, Parker I (1998). Kinetics of elementary Ca^{2+} puffs evoked in *Xenopus* oocytes by different Ins(1,4,5)P_3 receptor agonists. Biochem J 334: 505–509.

Marchant JS, Beecroft MD, Riley AM, Jenkins DJ, Marwood RD, Taylor CW *et al*. (1997a). Disaccharide polyphosphates based upon adenophostin A activate hepatic D-*myo*-inositol 1,4,5-trisphosphate receptors. Biochemistry 36: 12780–12790.

Marchant JS, Chang Y-T, Chung S-K, Irvine RF, Taylor CW (1997b). Rapid kinetic measurements of $^{45}Ca^{2+}$ mobilization reveal that Ins(2,4,5)P_3 is a partial agonist of hepatic InsP_3 receptors. Biochem J 321: 573–576.

Marwood RD, Riley AM, Correa V, Taylor CW, Potter BVL (1999). Simplification of adenophostin A defines a minimal structure for potent glucopyranoside-based mimics of D-*myo*-inositol 1,4.5.-trisphosphate. Bioorg Med Chem Lett 9: 453–458.

Marwood RD, Jenkins DJ, Correa V, Taylor CW, Potter BVL (2000). Contribution of the adenine base to the activity of adenophostin A investigated using a base replacement strategy. J Med Chem 43: 4278–4287.

Mochizuki T, Kondo Y, Abe H, Tovey SC, Dedos SG, Taylor CW *et al*. (2006). Synthesis of adenophostin A analogues conjugating an aromatic group at the 5′-position as potent IP_3 receptor ligands. J Med Chem 49: 5750–5758.

Morris SA, Nerou EP, Riley AM, Potter BVL, Taylor CW (2002). Determinants of adenophostin A binding to inositol trisphosphate receptors. Biochem J 367: 113–120.

Nerou EP, Riley AM, Potter BVL, Taylor CW (2001). Selective recognition of inositol phosphates by subtypes of inositol trisphosphate receptor. Biochem J 355: 59–69.

Ott RL, Longnecker M (2010). An introduction to statistical methods and data analysis. Brooks/Cole, Cengage Learning.

Parekh AB, Riley AM, Potter BVL (2002). Adenophostin A and ribophostin, but not inositol 1,4,5-trisphosphate or *manno*-adenophostin, activate a Ca^{2+} release-activated Ca^{2+} current, I_{CRAC}, in weak intracellular Ca^{2+} buffer. Biochem J 361: 133–141.

Potter BVL, Lampe D (1995). Chemistry of inositol lipid mediated cellular signaling. Angew Chem Int Ed Engl 34: 1933–1972.

Ramos-Franco J, Galvan D, Mignery GA, Fill M (1999). Location of the permeation pathway in the recombinant type-1 inositol 1,4,5-trisphosphate receptor. J Gen Physiol 114: 243–250.

Rosenberg HJ, Riley AM, Laude AJ, Taylor CW, Potter BVL (2003). Synthesis and Ca^{2+}-mobilizing activity of purine-modified mimics of adenophostin A: a model for the adenophostin-Ins(1,4,5)P_3 receptor interaction. J Med Chem 46: 4860–4871.

Rossi AM, Riley AM, Tovey SC, Rahman T, Dellis O, Taylor EJA *et al*. (2009). Synthetic partial agonists reveal key steps in IP_3 receptor activation. Nat Chem Biol 5: 631–639.

Rossi AM, Riley AM, Potter BVL, Taylor CW (2010). Adenophostins: high-affinity agonists of IP_3 receptors. Curr Top Membr 66 (in press)

Shuto S, Tatani K, Ueno Y, Matsuda A (1998). Synthesis of adenophostin analogues lacking the adenine moiety as novel potent IP_3 receptor ligands: some structural requirements for the significant activity of adenophostin A. J Org Chem 63: 8815–8824.

Sugawara H, Kurosaki M, Takata M, Kurosaki T (1997). Genetic evidence for involvement of type 1, type 2 and type 3 inositol 1,4,5-trisphosphate receptors in signal transduction through the B-cell antigen receptor. EMBO J 16: 3078–3088.

Sureshan KM, Truselle M, Tovey S, Taylor CW, Potter BVL (2008). 2-Position base-modified analogs of adenophostin A as high-affinity agonists of the D-*myo*-inositol trisphosphate receptor: *in vitro* evaluation and molecular modeling. J Org Chem 73: 1682–1692.

Sureshan KM, Riley AM, Rossi AM, Tovey SC, Dedos SG, Taylor CW *et al*. (2009). Activation of IP_3 receptors by synthetic bisphosphate ligands. Chem Commun 14: 1204–1206.

Takahashi M, Kagasaki T, Hosoya T, Takahashi S (1994a). Adenophostins A and B: potent agonists of inositol-1,4,5-trisphosphate receptor produced by *Penicillium brevicompactum*. Taxonomy, fermentation, isolation, physico-chemical and biological properties. J Antibiot 46: 1643–1647.

Takahashi M, Tanzawa K, Takahashi S (1994b). Adenophostins, newly discovered metabolites of *Penicillium brevicompactum*, act as potent agonists of the inositol 1,4,5-trisphosphate receptor. J Biol Chem 269: 369–372.

Takahashi S, Takeshi K, Takahashi M (1994c). Adenophostins A and B: potent agonists of inositol-1,4,5-trisphosphate receptors produced by *Penicillium brevicompactum*. Structure elucidation. J Antibiot 47: 95–100.

Tatani K, Shuto S, Ueno Y, Matsuda A (1998). Synthesis of 1-*O*-[3*S*,4*R*)-3-hydroxytetrahydrofuran-4-yl]-α-D-glucopyran oside 3,4,3′-trisphosphate as a novel potent IP_3 receptor ligand. Tetrahedron Lett 39: 5065–5068.

Taylor CW, Genazzani AA, Morris SA (1999). Expression of inositol trisphosphate receptors. Cell Calcium 26: 237–251.

Taylor CW, Fonseca PCA, Morris EP (2004). IP_3 receptors: the search for structure. Trends Biochem Sci 29: 210–219.

Tovey SC, Sun Y, Taylor CW (2006). Rapid functional assays of intracellular Ca^{2+} channels. Nat Protocol 1: 259–263.

Wilcox RA, Erneux C, Primrose WU, Gigg R, Nahorski SR (1995). 2-Hydroxy-α-D-glucopyranoside-2,3′,4′-trisphosphate, a novel, metabolically resistant, adenophostin A and *myo*-inositol-1,4,5-trisphosphate analogue, potently interacts with the *myo*-inositol-1,4,5-trisphosphate receptor. Mol Pharmacol 47: 1204–1211.

Yang X, Wang M, Fitzgerald MC (2004). Analysis of protein folding and function using backbone modified proteins. Bioorg Chem 32: 438–449.

Yoshida M, Sensui N, Inoue T, Morisawa M, Mikoshiba K (1998). Role of two series of Ca^{2+} oscillations in activation of ascidian eggs. Dev Biol 203: 122–133.

Yoshikawa F, Morita M, Monkawa T, Michikawa T, Furuichi T, Mikoshiba K (1996). Mutational analysis of the ligand binding site of the inositol 1,4,5-trisphosphate receptor. J Biol Chem 271: 18277–18284.

Supporting information

Additional Supporting Information may be found in the online version of this article:

Table S1 Relative potencies and affinities of IP_3 and AdA analogues interacting with native IP_3R1 and its N-terminal fragments. The table shows the relative effectiveness for each pair of ligands in evoking Ca^{2+} release from DT40-IP_3R1 cells (ΔpEC_{50}) and in binding (in TEM) to full-length IP_3R1 and NT, and binding (in CLM) to the NT or IBC (ΔpK_d). Results are shown as means ± SEM, from at least three independent experiments. The data from which these values are derived are shown in Figure 2.

Table S2 Relative affinities of IP_3 and AdA analogues interacting with wild-type and mutant IBC. For each ligand, the relative affinity (ΔpK_d) is shown for mutant and wild-type IBC (in CLM). Results are shown as means ± SEM, from at least three independent experiments. The data from which these values are derived are shown in Figures 2, 3 and 4.

Table S3 Relative potencies of IP_3 and AdA analogues interacting with mutant IP_3R1. For each ligand the relative potency in evoking Ca^{2+} release (ΔpEC_{50}) is shown for wild-type and mutant IP_3R. Results are shown as means ± SEM, from at least three independent experiments. The data from which these values are derived are shown in Figures 2, 3 and 4.

Please note: Wiley-Blackwell are not responsible for the content or functionality of any supporting materials supplied by the authors. Any queries (other than missing material) should be directed to the corresponding author for the article.